The International Journal of Advanced Manufacturing Technology (2019) 103:1199–1209
https://doi.org/10.1007/s00170-019-03624-2

ORIGINAL ARTICLE

Electric hot incremental sheet forming of Ti-6Al-4V titanium, AA6061 aluminum, and DC01 steel sheets

Mostafa Vahdani[1] · Mohammad Javad Mirnia[1] · Mohammad Bakhshi-Jooybari[1] · Hamid Gorji[1]

Received: 2 September 2018 / Accepted: 20 March 2019 / Published online: 2 April 2019

Abstract
Single point incremental forming (SPIF) is an emerging forming process for rapid prototyping and manufacturing of complex components from sheet metals. Recently, the use of electric current for the local resistance heating of the deformation area has attracted much attention in SPIF. In order to further study the electric hot incremental sheet forming (EHISF), in the present research, the effect of utilizing various lubricants on the formability of Ti-6Al-4V, AA6061, and DC01 sheet metals is experimentally investigated by forming a truncated cone under different feed rates, vertical pitches, and electric currents. To this end, the Taguchi design of experiment (DOE) and the analysis of variance (ANOVA) are employed. The results showed that the formability of Ti-6Al-4V and AA6061 sheets can be improved using the EHISF. For both the sheets, the lubricant and the electric current have significant effects on the maximum achievable forming depth. In addition, the formability of the DC01 sheet is highly affected by the lubricant and the feed rate. The results of the DC01 sheet showed that at the considered wall angle, the maximum forming depth in the EHISF does not change, compared to the cold SPIF, but the thickness distribution of the formed part at a higher temperature is more uniform.

Keywords Incremental sheet forming (ISF) · Hot forming · Electrically assisted manufacturing · Lubrication condition · Formability

1 Introduction

Sheet metals with a high strength-to-weight ratio, such as some aluminum, titanium, and magnesium alloys, have a low formability at room temperature. One of the emerging processes for forming these alloy sheets is the single point incremental forming (SPIF) at elevated temperatures which needs no dedicated dies and has low initial cost in rapid prototyping or small batch production. In SPIF, a hemispherical head tool gradually and locally pushes the sheet along a specified tool path. The tool path is extracted according to the desired geometry and is usually applied to the forming tool using a CNC milling machine [1].

The high-temperature SPIF can be carried out by locally heating up the deformation zone or uniformly elevating the temperature of the entire sheet. The dynamic local heating can be provided using a laser source [2], the electrical resistance of the contact area between the sheet and the forming tool due to a high current [3], the frictional heat caused by a high rotational speed of the forming tool [4], or an induction electric current [5]. Usually, the global heating of the sheet is carried out by heating elements [6, 7].

Because in SPIF only a small area below the forming tool undergoes the plastic deformation [8], the local heating method has been much studied in the literature. Among the abovementioned local heating methods, electric hot incremental sheet forming (EHISF) can be considered as a flexible and simple process. This simplicity and flexibility are mainly due to the fact that the EHISF process does not need any extra controller to separately move the external heating source. In this method, an electric power supply (transformer) is added to the conventional equipment of cold SPIF and a high electric current with a low voltage passes through the forming tool and the sheet. Then, based on the Joule law, the localized deformation zone is heated by receiving the thermal energy Q [9]:

$$Q = RtI^2 \tag{1}$$

✉ Mohammad Javad Mirnia
mirnia@nit.ac.ir

[1] Mechanical Engineering Department, Babol Noshirvani University of Technology, Babol 47148-71167, Iran

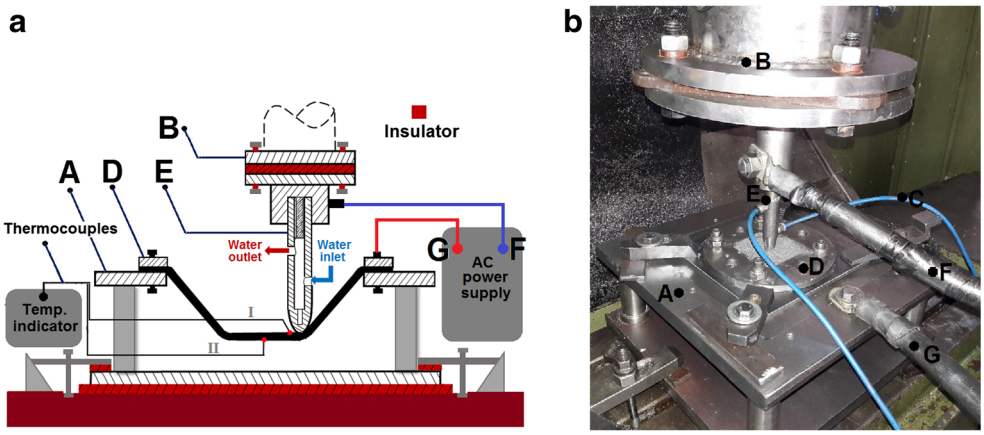

Fig. 1 **a** The scheme of EHISF and **b** the experimental equipment used in the experiments (A, base structure; B, tool holder; C, cooling system; D, blank holder; E, forming tool; F, Anode +; G, cathode −)

where R, t, and I are the electrical resistance of the contact area, the contact duration, and the electric current, respectively.

Ti-6Al-4V sheet was formed using EHISF by Fan et al. [10] at the temperature range of 500–600 °C. To improve the surface finish and prevent the oxidation, a 20-μm-thick layer of the Ni–MoS_2 composite was applied to the sheet. The results showed that in this temperature range, the titanium sheet is formed with a higher dimensional accuracy. Ambrogio et al. [11] carried out EHISF of a truncated cone of AZ31B-O magnesium, Ti-6Al-4V titanium, and AA2024-T3 aluminum sheets at different wall angles. It was concluded that an optimum value exists for the electric current. Shi et al. [12] improved the dimensional accuracy of a low carbon steel sheet using EHISF and MoS_2 powder as the lubricant. Two heating techniques, namely the resistance and frictional stir heating, were implemented by Xu et al. [4] in SPIF of the AZ31 magnesium sheet. It was stated that the resistance heating can raise the sheet temperature much faster and, thus, is less dependent on the geometry of the part. Xu et al. [13] investigated the surface roughness and dimensional accuracy of AZ31B magnesium sheets by using electrically assisted double-sided incremental forming (E-DSIF). The results showed that the dimensional accuracy and surface finish are improved using E-DSIF process. Using EHISF, Honarpisheh et al. [14] formed a titanium alloy sheet with the MoS_2 powder as the lubricant. They concluded that the thinning of the formed part increases by increasing the wall angle and by decreasing the vertical pitch. They also stated that the forming force increases by increasing the vertical pitch and decreasing the tool diameter. Najafabady and Ghaei [15] experimentally studied EHISF of the Ti-6Al-4V sheet to determine the effect of the lubrication condition, the initial thickness, and the vertical pitch on the dimensional accuracy and surface finish. Liu et al. [16] developed forming tools with a cooling system to reduce the tool surface wear and to improve the surface finish of the final part in EHISF of the Ti-6Al-4V sheet. The copper-based anti-seize lubricant was utilized during EHISF. Magnus [17] performed EHISF of the Ti-6Al-4V sheet using a precise temperature control and measurement to reduce the surface wear of the forming tool tip and the formed part. Pacheco and Silveira [18] conducted a numerical simulation to investigate EHISF of AA1050 aluminum alloy with and without preheating. The results revealed that preheating the aluminum sheet results in a decline in the forming force.

The success of the EHISF process is highly dependent on the type of initial material. Compared to the Ti-6Al-4V titanium sheet, EHISF of AA6061 and DC01 sheets has been less studied in the literature. The present research systematically investigates the EHISF process of Ti-6Al-4V titanium, AA6061 aluminum, and DC01 steel sheets. In addition to the conventionally used lubricants, namely graphite and

Table 1 EHISF parameters and their respective levels for each sheet metal

Notations	Parameters	Unit	No. of levels	Level			
				1	2	3	4
I	Current	A	2	450	300	–	–
F	Feed rate	mm/min	2	900	400	–	–
P	Vertical pitch	mm	2	0.3	0.2	–	–
L	Lubricant	–	4	Graphite	Graphite-based anti-seize	MoS2	Copper-based anti-seize

Table 2 Design matrix of experiments using the Taguchi L_8 orthogonal array

Test no.	*L*	*F*	*P*	*I*
1	1	1	1	1
2	1	2	2	2
3	2	1	1	2
4	2	2	2	1
5	3	1	2	1
6	3	2	1	2
7	4	1	2	2
8	4	2	1	1

MoS_2 powders, here, the influence of the graphite-based and copper-based anti-seize lubricants is investigated. Effects of feed rate, vertical pitch, and electric current on the maximum achievable forming depth are experimentally studied.

2 Materials and methods

2.1 Experimental equipment of EHISF

EHISF process, as schematically shown in Fig. 1a, is studied in the present research. A three-axis CNC milling machine together with the experimental equipment shown in Fig. 1b was utilized to perform the SPIF process. An AC transformer was employed as the power supply with the output current and voltage in the range of 300–1000 A and 1–5 V. Using electrical cables, the blank and the hemispherical head tool were connected to the negative and positive poles of the power supply, respectively. The phenolic resin cotton sheet was utilized to electrically insulate the CNC machine from the electric current, as illustrated in Fig. 1a. In order to maintain the rigidity of the tool and also to avoid an early tool tip wear at high temperatures, which has a negative effect on the formability of the sheet metal, the forming tool should always be kept at a low temperature during EHISF. To this end, a cooling channel for water flow was drilled into the forming tool, as depicted in Fig. 1a.

The hemispherical head forming tool with the diameter of 10 mm was made from hot work tool steel. The feed rate, electric current, and vertical pitch were set according to the design of experiment (DOE) matrix. The SPIF process was carried out without spindle rotational speed. The spiral tool path was utilized to SPIF the test geometry. Two K-type thermocouples were used to measure the temperature of the region near the contact zone and the part bottom, as schematically shown in Fig. 1a. During the tests, only the maximum temperature measured using the thermocouples is reported. To continuously record the forming zone temperature during the EHISF process, the approaches developed in the literature, like the one proposed by Min et al. [9], can be implemented.

In forming at high temperatures, an appropriate lubrication depending on the heating method is essential to reduce the friction and prevent a premature sheet fracture and tool wear. In EHISF, solid lubricants such as MoS_2 and graphite powders are frequently used. Besides these solid lubricants, copper-based and graphite-based anti-seize compounds are also utilized to investigate their effects on the formability of the considered sheet metals. The surface of the blank was uniformly covered by a desired lubricant before performing EHISF.

Considering the Joule law, Eq. (1), the electric current directly affects the generated heat and the local temperature rise at the contact zone. The feed rate determines the contact duration at a specific point in Eq. (1). It was theoretically illustrated by Mirnia and Mollaei [8] that the extent of the deformation field and the contact zone is affected by the vertical pitch. The extent of the contact zone specifies the electrical resistance between the forming tool and the sheet in Eq. (1). Accordingly, the temperature elevation in the deformation region is affected by the vertical pitch. Hence, effects of feed rate, vertical pitch, and electric current on formability are also studied.

A Mahr mobile roughness measuring instrument was used to measure the average surface roughness (R_a). The amount of the tool tip wear was measured as the height reduction of the tool after the forming process by means of a tool presetter (a measuring instrument associated with CNC machine tools) with an accuracy of 0.01 mm. For each experiment, a fresh forming tool was used to precisely measure the amount of the tool wear in the considered experiment.

2.2 Taguchi design of experiments

Table 1 lists the parameters and their respective levels investigated in the present study. Some preliminary trial and error-based experiments were conducted to choose appropriate levels for each parameter. During the preliminary

Table 3 The physical and mechanical properties of the investigated sheets at room temperature

Sheet	Density (g/cm^3)	Electrical resistivity (Ω cm)	Thermal conductivity (W/m K)	Young's modulus (GPa)	Yield strength (MPa)	Ultimate strength (MPa)	Uniform elongation (%)
DC01	6.9	1.59×10^{-5}	51.9	210	280	440	28
Ti-6Al-4V	4.5	1.78×10^{-4}	6.7	120	920	950	18
AA6061	2.7	3.66×10^{-6}	167.0	69	276	310	12

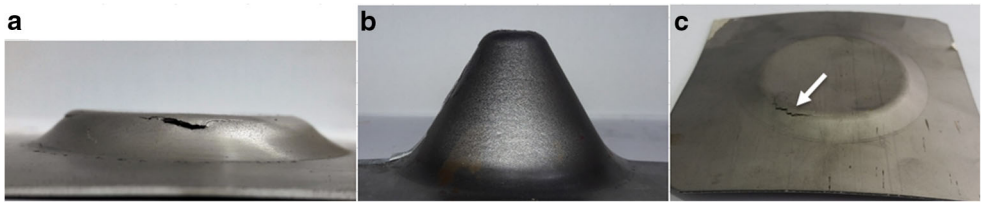

Fig. 2 Truncated cones formed at room temperature. **a** AA6061. **b** DC01. **c** Ti-6Al-4V parts

experiments, the possibility of forming parts with acceptable appearance has been considered. It should be mentioned that if the parameters of the EHISF process are adjusted outside certain ranges, parts with an unacceptable appearance can result from sparks and excessive local heating. Regarding these different levels for the investigated parameters, the Minitab software suggested both the L_8 and L_{16} orthogonal arrays. The L_8 array was implemented in the present study, as presented in Table 2. Each experiment was repeated two times and the fracture depth as a formability indicator was measured. Regarding Table 2, 16 experimental runs were carried out. The analysis of variance (ANOVA) and the signal-to-noise ratio (*S*/*N*) were implemented within the Minitab environment to determine significant parameters on the forming depth based on the statistical analysis of the experimental results in EHISF of each sheet metal. The *S*/*N* ratio was calculated according to the quality characteristic of "the larger is the better."

2.3 Materials

The present research considers SPIF of Ti-6Al-4V, AA6061, and DC01 alloy sheets with the initial thickness of 1 mm. Ti-6Al-4V and AA6061 sheets have been considered due to their high strength-to-weight ratio and low formability at room temperature. On the other hand, due to its good formability at room temperature, the DC01 sheet has been considered to investigate any possible destructive effect of the EHISF process on the formability. Uniaxial tension tests along the rolling direction were conducted to obtain the mechanical properties, as presented in Table 3. The physical properties of the considered sheets are also depicted in Table 3. A 60° wall angle cone with the base diameter of 58 mm was chosen as the test geometry. The dimensions of the initial blanks were 100 mm × 100 mm.

3 Results and discussion

3.1 SPIF at room temperature

The SPIF process of Ti-6Al-4V, AA6061, and DC01 sheets was carried out at room temperature using MoS_2 lubricant. Figure 2 shows the formed parts at the fracture depth. The fracture depth of the aluminum part was obtained as 7.56 mm. The DC01 sheet was successfully formed up to the designed depth of 35 mm. The titanium sheet was fractured at the depth of 3.25 mm. As can be seen from Fig. 2c, besides the low formability at room temperature, the titanium part shows a large springback after unclamping.

3.2 Parameters study on the formability in EHISF

The fracture depth in each repetition, the respective *S*/*N* ratio, and the mean value are listed in Table 4 for the considered

Table 4 Fracture depths together with *S*/*N* ratios

Test no.	Fracture depth (mm)											
	Ti-6Al-4V				AA6061				DC01			
	Repetition		*S*/*N* ratio	Mean	Repetition		*S*/*N* ratio	Mean	Repetition		*S*/*N* ratio	Mean
	I	II			I	II			I	II		
1	35.00	35.00	30.88	35.00	6.02	5.96	15.55	5.99	33.21	33.15	30.41	33.18
2	6.32	6.19	15.92	6.25	7.53	7.48	17.50	7.50	32.12	32.18	30.14	32.14
3	7.48	7.32	17.38	7.40	7.41	7.45	17.41	7.43	35.00	35.00	30.88	35.00
4	12.84	13.12	22.26	12.98	3.43	3.38	10.64	3.40	28.34	28.41	29.05	28.37
5	9.73	10.14	19.93	9.93	4.93	4.97	13.89	4.95	22.17	22.09	26.88	22.13
6	8.46	8.28	18.45	8.37	6.73	6.65	16.50	6.69	12.81	12.92	22.18	12.86
7	7.34	7.52	17.41	7.43	8.91	9.08	19.07	8.99	35.00	35.00	30.88	35.00
8	7.98	7.83	17.95	7.90	3.94	3.79	11.73	3.86	11.48	11.53	21.21	11.50

Table 5 ANOVA results for the formability of the Ti-6Al-4V titanium sheet

Factor	DOF	Sum of squares	Variance	*F* ratio	Pure sum	Contribution (%)
L	3	418.223	139.407	4.811	331.300	25.913
F	1	147.076	147.076	5.076	118.101	9.237
P	1	121.826	121.826	4.204	92.852	7.262
I	1	330.603	330.603	11.410	301.629	23.592
Error	9	260.767	28.974			
Total	15	1278.497				

Table 6 ANOVA results for the formability of the AA6061 aluminum sheet

Factor	DOF	Sum of squares	Variance	*F* ratio	Pure sum	Contribution (%)
L	3	4.293	1.431	26.925	4.133	7.924
F	1	8.706	8.706	163.821	8.653	16.589
P	1	0.192	0.192	3.629	0.139	0.267
I	1	38.492	38.492	724.248	38.439	73.689
Error	9	0.477	0.053			
Total	15	52.163				

Table 7 ANOVA results for the formability of the DC01 steel sheet

Factor	DOF	Sum of squares	Variance	F ratio	Pure sum	Contribution (%)
L	3	625.216	208.405	100.505	618.995	47.322
F	1	408.352	408.352	196.931	406.278	31.06
P	1	157.558	157.558	75.983	155.484	11.886
I	1	98.251	98.251	47.382	96.178	7.352
Error	9	18.661	2.073			
Total	15	1308.04				

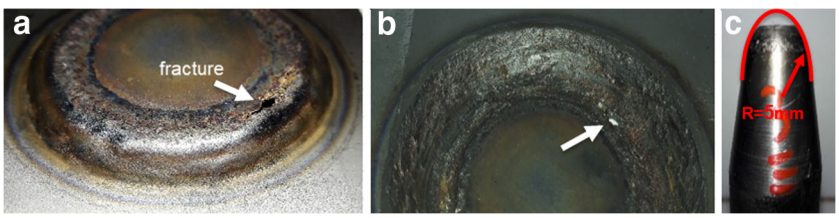

Fig. 3 The titanium part formed in experiment no. 7. **a** The outer appearance. **b** The inner surface. **c** The tool tip wear

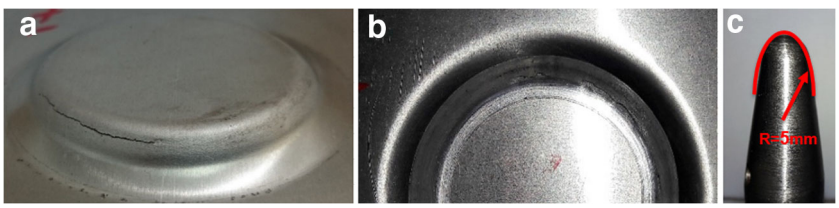

Fig. 4 The aluminum formed part in experiment no. 7. **a** The outer appearance. **b** The inner surface. **c** The tool tip wear

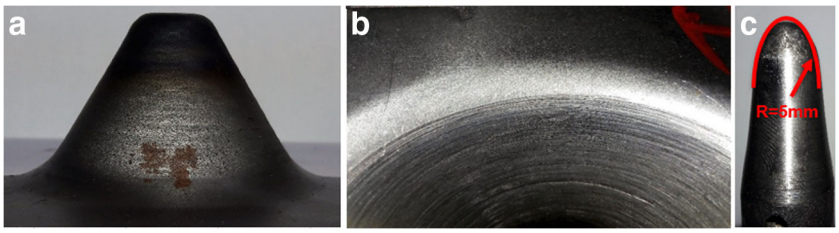

Fig. 5 The steel formed part in experiment no. 7. **a** The outer appearance. **b** The inner surface. **c** The tool tip wear

materials according to the design matrix of Table 2. In EHISF of the titanium, aluminum, and steel sheets, the maximum achievable forming depths are 35, 9, and 35 mm, and the minimum ones are 6.25, 3.40, and 11.50 mm, respectively. As seen in Table 4 for the DC01 sheet, the maximum forming depth of 35 mm was achieved through both experiment no. 3 and no. 7. The smallest and largest forming depths achieved using EHISF are compared to the one attained in cold SPIF. As can be found from Table 4, the fracture depth of the titanium sheet for all parameter combinations is higher than the one in cold SPIF. The smallest fracture depth obtained in experiment no. 2 is 92% higher than the one in cold SPIF. For the other two materials, a smaller fracture depth than that of cold SPIF was achieved by some experiments. For the aluminum and steel sheets, the forming depth is reduced by 55% (experiment no. 4) and 67% (experiment no. 8) compared to cold SPIF, respectively. The results show that an appropriate parameter setting for EHISF is a critical issue which significantly depends on the considered material.

The percentage contribution of each investigated parameter on formability was analyzed using ANOVA and is presented in Tables 5, 6, and 7 for Ti-6Al-4V, AA6061, and DC01 sheets, respectively. According to Table 5, the lubricant and the electric current with the percentage contribution of 26% and 24%, respectively, are the dominant factors affecting the formability of the titanium sheet. The significant role of the lubricant in the formability of the titanium sheet can be inferred from the work of Fan et al. [10]. Also, Ambrogio et al. [11] demonstrated that there is an optimum value for the electric current to successfully perform EHISF of the titanium sheet, which highlights the importance of the current. ANOVA results for the aluminum sheet (Table 6) revealed that the electric current with the contribution of 74% is the most effective parameter on the formability. Regarding Table 7, the formability of the DC01 sheet is most strongly affected by the lubricant followed by the feed rate with the percentage contribution of 47% and 31%, respectively.

Based on Table 4, the titanium sheet is successfully formed up to the designed depth in experiment no. 1. Also, the highest formability for the aluminum sheet is obtained through experiment no. 7. On the other hand, all three sheets have been formed up to a relatively moderate depth during experiment no. 5 compared to the other experiments. In the following, further investigations are focused on experiment no. 1, no. 5, and no. 7 to compare the fracture depth, the tool wear, and the surface roughness in SPIF of the considered materials.

3.2.1 Experiment no. 7

Figure 3 illustrates the titanium part at the fracture depth and the effect of the spark on its surface in experiment no. 7. During EHISF of the titanium sheet at the lower current of 300 A and at the higher feed rate of 900 mm/min, the grease of the copper-based anti-seize compound evaporated and only the copper particles remained. This resulted in electric sparks and, consequently, led to a local melting of the sheet surface and a premature fracture (at the forming depth of 7.43 mm). Also, due to the small cavities created on the inner surface of the truncated cone and the tool tip, the obtained surface finish was undesirable and an excessive abrasion of the tool occurred. The surface roughness and the tool wear measured in experiment no. 7 for Ti-6Al-4V sheet are respectively 5.12 μm and 1.63 mm, as can be qualitatively seen in Fig. 3b, c. The value of the surface roughness of Ti-6Al-4V sheet is considerably better than the one obtained by Liu et al. [16]. In their investigation, the surface roughness of the Ti-6Al-4V sheet was equal to 15.11 μm by utilizing the copper-based anti-seize lubricant.

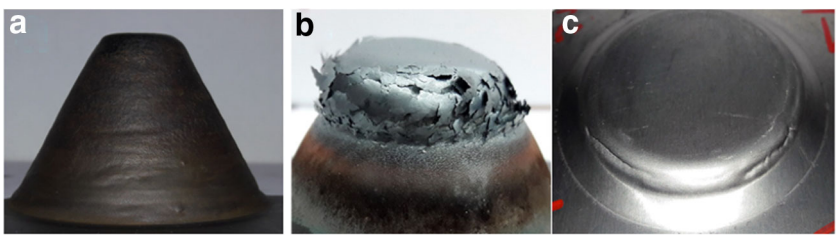

Fig. 6 The specimens formed in experiment no. 1. **a** Ti-6Al4V titanium. **b** DC01 steel. **c** AA6061 aluminum sheets

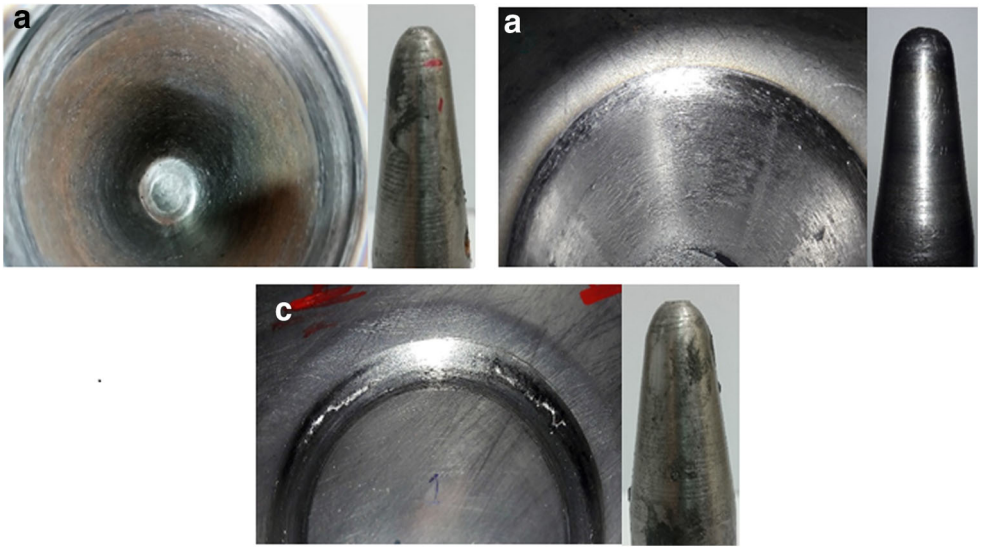

Fig. 7 The inner surface and the abrasion of the forming tool in experiment no. 1. **a** Ti-6Al4V titanium. **b** DC01 steel. **c** AA6061 aluminum sheets

The highest forming depth of the AA6061 sheet achieved in experiment no. 7 is equal to 8.99 mm, as presented in Table 4. The maximum measured temperature of the aluminum sheet was 86 °C and no electric spark appeared during this test. Accordingly, as seen in Fig. 4, a proper surface roughness of 1.24 μm was obtained. Also, the amount of the tool wear illustrated in Fig. 4c was very small, equal to 0.06 mm. The steel part shown in Fig. 5 was successfully formed up to 35 mm depth using the parameter combination of experiment no. 7. Figure 7b, c shows the surface finish and tool wear in this test. During this experiment, the measured temperature of the steel sheet was about 380 °C with no evidence of electric spark. As depicted in Fig. 5b, c, the tool wear and the surface roughness were measured as 0.08 mm and 2.30 μm, respectively.

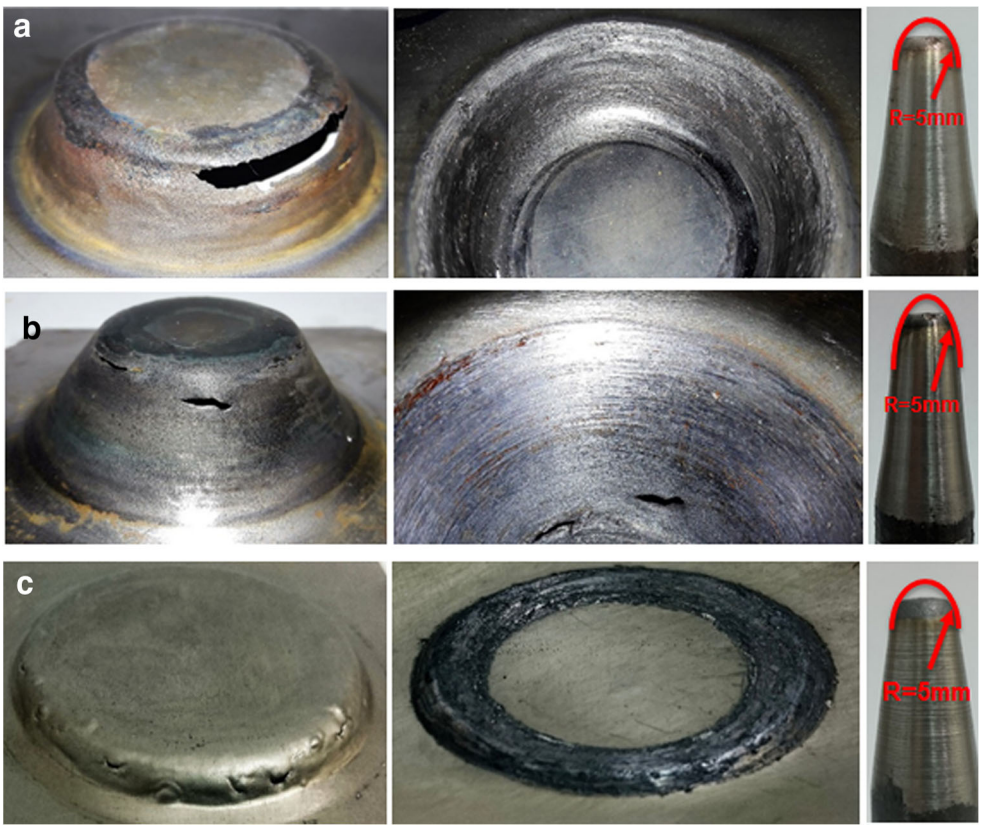

Fig. 8 The outer and inner surfaces of the formed specimens and the abrasion of the forming tool in experiment no. 5. **a** Ti-6Al4V titanium. **b** DC01 steel. **c** AA6061 aluminum sheets

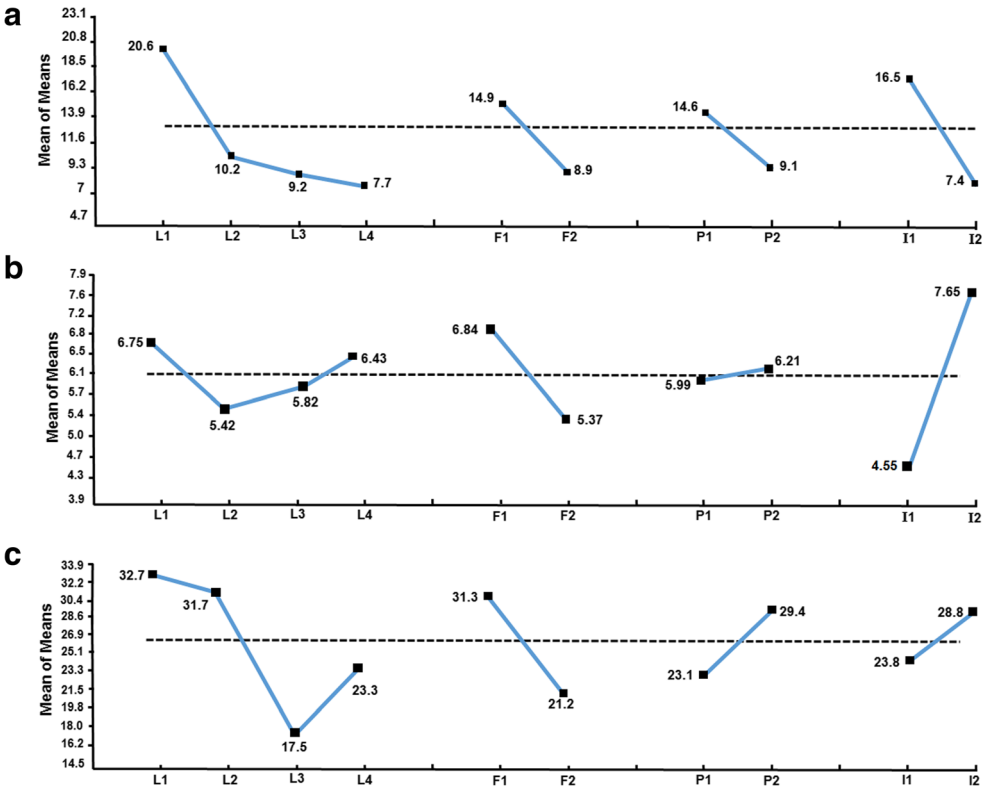

Fig. 9 The main effects plot for the forming depth of the sheet. **a** Ti-6Al-4V. **b** AA6061. **c** DC01

3.2.2 Experiment no. 1

In experiment no. 1, graphite powder was employed as the lubricant and was properly placed on the contact zone. Graphite powder particles did not stick to each other under the highest level of the current and feed rate (Table 2). The truncated cones formed in experiment no. 1 are depicted in Fig. 6. Regarding Table 4, the formability of the titanium sheet under the parameter combination utilized in experiment no. 1 is the highest and the formability of the steel sheet is appropriate. The steel sheet temperature was raised to 860 °C under which oxide layers were formed on the outer surface of the part, as shown in Fig. 6b. The titanium part temperature reached 750 °C. Figure 7 illustrates the inner surface of the formed parts and the abrasion of the forming tools during experiment no. 1. The surface roughness of the titanium sheet which was successfully formed up to 35 mm depth is 4.52 μm, and the amount of the tool wear shown in Fig. 7a is 0.12 mm. Regarding these results, it is obvious that by using the graphite powder, no sparks took place in the present study. However, Fan et al. [10] stated that spark appeared in the tool-sheet contact zone during their EHISF process of a titanium sheet using graphite powder. The surface roughness and the tool wear of the steel part depicted in Fig. 7b are 1.69 μm and 0.10 mm, respectively. Due to the small forming depth, the surface roughness of the aluminum sheet (Fig. 7c) could not be precisely measured, but the tool wear was obtained as 0.09 mm.

3.2.3 Experiment no. 5

Figure 8 indicates the fractured specimens, their inner surfaces, and the forming tools worn at the end of experiment no. 5. After this experiment, for all materials, the curvature of the forming tool head is lost due to the severe abrasion. By using the MoS_2 powder for the titanium blank, the burning of

Table 8 Fracture depth obtained using the optimal combination of the parameters and the confirmation tests

Material	Optimal combination					Fracture depth (mm)		Surface roughness (μm)	Tool wear (mm)	Temperature (°C)
		Lubricant	Feed rate (mm/min)	Vertical pitch (mm)	Current (A)	Predicted	Experimental			
Ti-6Al-4V	L1 F1 P1 I1	Graphite	900	0.3	450	32.96	35.00	4.52	0.12	750
AA6061	L1 F1 P2 I2	Graphite	900	0.2	300	9.14	9.17	1.12	0.14	95
DC01	L1 F1 P2 I2	Graphite	900	0.2	300	43.33	35.00	1.75	0.07	430

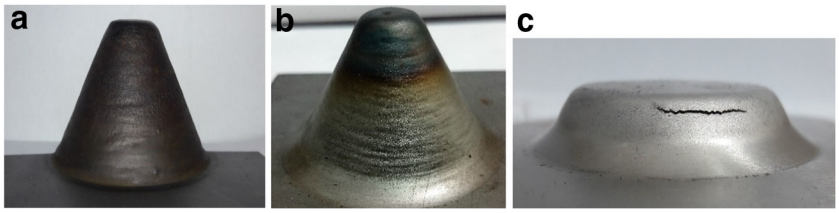

Fig. 10 The specimens formed using the optimal parameter combinations. **a** Ti-6Al4V. **b** DC01. **c** AA6061

the lubricant followed by the sheet burning occurred, which resulted in an early fracture initiation at a depth of 9.93 mm, as shown in Fig. 8a. At elevated temperatures, the MoS_2 powder was strongly bonded to the inner surface of the titanium sheet such that it cannot be easily removed after EHISF. Accordingly, a surface roughness of 9.64 μm was achieved for the titanium part, and the forming tool shown in Fig. 8a was excessively worn by the amount of 1.27 mm.

In experiment no. 5 for the aluminum sheet, sparks together with local melting took place at the tool contact zone with the sheet, which caused a significant tool wear as well as an undesirable surface finish, as can be seen in Fig. 8c. Consequently, a small forming depth equal to 4.95 mm was attained. The abrasion of the tool head occurring during SPIF of the aluminum sheet in experiment no. 5 is 1.38 mm, which is significant with respect to the small forming depth, as compared to the tool wear occurred in SPIF of the titanium and steel sheets with larger forming depths.

Under the condition of experiment no. 5, the DC01 steel sheet was formed up to a relatively higher forming depth equal to 22.17 mm as compared to two other materials. In this test, a maximum temperature of about 580 °C was measured for the steel sheet. Although no electric sparks appeared during the test, the MoS_2 powder resulted in a poor surface finish of the steel cone such that its surface roughness is 3.16 μm. The tool wear for the steel specimen is 1.13 mm, as depicted in Fig. 8b.

3.3 Optimum combination of parameters

Figure 9 shows the main effects plot for the forming depth in EHISF of Ti-6Al-4V, AA6061, and DC01 sheets. Based on the main effects plot, the optimum combination of the parameters maximizing the formability can be suggested for each material as presented in Table 8. EHISF of the considered materials using the respective optimum parameter combination was experimentally performed to evaluate the predicted values by the Taguchi method. As seen in Table 8, the fracture depths obtained in the confirmation tests are in agreement with the predicted values. It should be noted from Table 8 that the predicted fracture depth for the DC01 sheet is higher than the maximum forming depth of 35 mm which can be geometrically obtained in the investigated truncated cone.

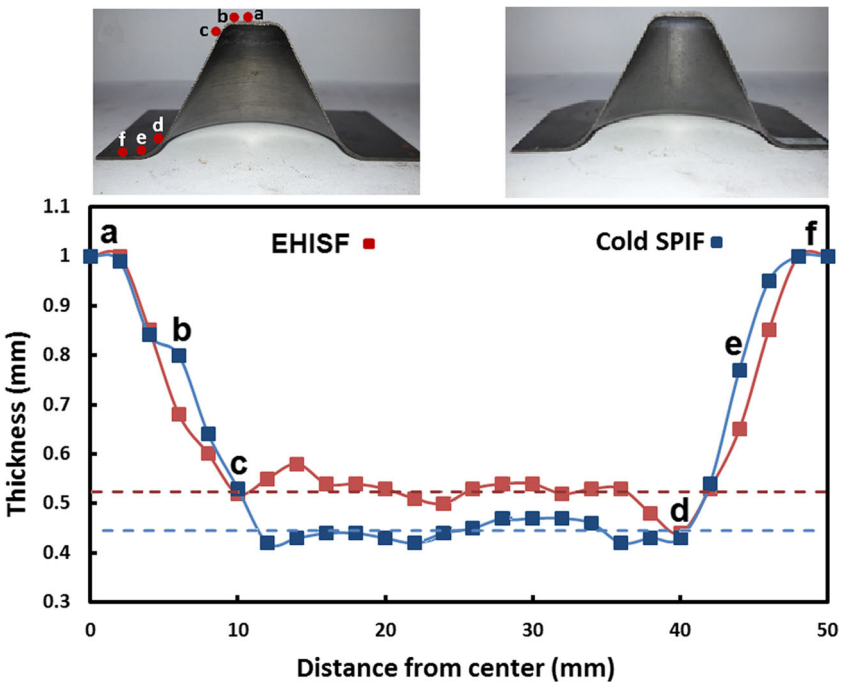

Fig. 11 The thickness distribution in the steel truncated cone formed by cold SPIF and EHISF under the optimal parameter combination (graphite, 900 mm/min, 0.2 mm, and 300 A)

With respect to Table 8, EHISF using the optimal parameter setting can significantly improve the forming depth of the titanium sheet from 3.25 mm in cold SPIF to 35 mm in high temperature forming. Only a small improvement of 21% in the forming depth of the aluminum sheet has resulted from EHISF. In cold SPIF of the steel sheet, the maximum designed depth is successfully achieved and no further improvement in the forming depth would be expected by EHISF due to the design constraint of the considered cone. In EHISF using the optimal parameters, the surface roughness values were 4.52, 1.12, and 1.75 μm, and also the amount of the abrasion of the forming tool was measured as 0.12, 0.14, and 0.07 mm for the Ti-6Al-4V, AA6061, and DC01 cones, respectively. Figure 10 indicates the formed specimens using the optimum parameters maximizing the formability.

3.4 Thickness distribution of DC01 steel sheet

As indicated in the "SPIF at room temperature" section, the DC01 steel sheet can be successfully formed up to the designed depth by means of cold SPIF. Regarding Table 8, it is expected that EHISF would be able to form the steel sheet up to a larger depth than 35 mm if there was no geometrical restriction due to the dimensions of the test geometry. The effect of EHISF on the steel sheet has been further investigated by comparing the sheet thickness distribution obtained in cold and high temperature forming. Figure 11 shows the sheet thickness distribution of the DC01 steel sheet formed up to the maximum height of 35 mm at room temperature compared to the sheet formed at high temperature using the optimal parameter combination in Table 8. It is evident from Fig. 11 that EHISF improved the thinning in the wall of the cone (region between points d and c). The average wall thickness in cold SPIF is 0.44 mm, while it increases to 0.52 mm in EHISF. In other words, an approximately 18% enhancement in the thickness distribution at the wall area has been achieved using EHISF. The thickness distribution at the bottom of the cone and the flange area has not been significantly affected in both processes.

4 Conclusions

The main goal of the present paper was to evaluate the formability improvement of the Ti-6Al-4V, AA6061, and DC01 sheets using EHISF. The influence of four process parameters, namely lubricant type, current intensity, pitch size, and feed rate, on the fracture depth as a formability indicator was statistically investigated through the Taguchi DOE and the ANOVA method. It can be concluded that:

- The formability of Ti-6Al-4V titanium sheet significantly depends on the lubricant type and the electric current value. The electric current was the most effective parameter on the formability of AA6061 sheet. In EHISF of DC01 sheet, the formability was mainly affected by the lubricant type and the feed rate.
- The optimal parameter combinations yielding maximum formability were obtained as graphite, 900 mm/min, 0.3 mm, and 450 A for the titanium sheet and graphite, 900 mm/min, 0.2 mm, and 300 A for both the aluminum and DC01 sheets. Using these optimal parameters, the formability of the Ti-6Al-4V and AA6061 sheets was improved, but the maximum forming depth of the DC01 sheet remained unchanged compared to the cold SPIF.
- Using EHISF under the optimal parameter combination, the wall thickness distribution of the DC01 sample was improved by 18% compared to the cold SPIF.

As a future work, microstructural evolutions during the EHISF process will be investigated under different process parameters to get more insight into the deformation mechanics. Also, the effects of process parameters on the temperature distribution will be studied in detail using more precise measuring instruments.

Compliance with ethical standards

Conflict of interest The authors declare that they have no conflict of interest.

References

1. Shamsari M, Mirnia MJ, Elyasi M, Baseri H (2018) Formability improvement in single point incremental forming of truncated cone using a two-stage hybrid deformation strategy. Int J Adv Manuf Technol 94(5):2357–2368. https://doi.org/10.1007/s00170-017-1031-5
2. Duflou JR, Callebaut B, Verbert J, De Baerdemaeker H (2007) Laser assisted incremental forming: formability and accuracy improvement. CIRP Ann 56(1):273–276. https://doi.org/10.1016/j.cirp.2007.05.063
3. Fan G, Gao L, Hussain G, Wu Z (2008) Electric hot incremental forming: a novel technique. Int J Mach Tools Manuf 48(15):1688–1692. https://doi.org/10.1016/j.ijmachtools.2008.07.010
4. Xu D, Lu B, Cao T, Chen J, Long H, Cao J (2014) A comparative study on process potentials for frictional stir- and electric hot-assisted incremental sheet forming. Procedia Engineering 81:2324–2329. https://doi.org/10.1016/j.proeng.2014.10.328
5. Al-Obaidi A, Kräusel V, Landgrebe D (2016) Hot single-point incremental forming assisted by induction heating. Int J Adv Manuf Technol 82(5):1163–1171. https://doi.org/10.1007/s00170-015-7439-x
6. Ambrogio G, Filice L, Manco GL (2008) Warm incremental forming of magnesium alloy AZ31. CIRP Ann 57(1):257–260. https://doi.org/10.1016/j.cirp.2008.03.066
7. Palumbo G, Brandizzi M (2012) Experimental investigations on the single point incremental forming of a titanium alloy component combining static heating with high tool rotation speed. Mater Des 40:43–51. https://doi.org/10.1016/j.matdes.2012.03.031

8. Mirnia MJ, Dariani BM (2012) Analysis of incremental sheet metal forming using the upper-bound approach. Proc Inst Mech Eng B J Eng Manuf 226(8):1309–1320. https://doi.org/10.1177/0954405412445113
9. Min J, Seim P, Störkle D, Thyssen L, Kuhlenkötter B (2017) Thermal modeling in electricity assisted incremental sheet forming. Int J Mater Form 10(5):729–739. https://doi.org/10.1007/s12289-016-1315-6
10. Fan G, Sun F, Meng X, Gao L, Tong G (2010) Electric hot incremental forming of Ti-6Al-4V titanium sheet. Int J Adv Manuf Technol 49(9):941–947. https://doi.org/10.1007/s00170-009-2472-2
11. Ambrogio G, Filice L, Gagliardi F (2012) Formability of lightweight alloys by hot incremental sheet forming. Mater Des 34:501–508. https://doi.org/10.1016/j.matdes.2011.08.024
12. Shi X, Gao L, Khalatbari H, Xu Y, Wang H, Jin L (2013) Electric hot incremental forming of low carbon steel sheet: accuracy improvement. Int J Adv Manuf Technol 68(1):241–247. https://doi.org/10.1007/s00170-013-4724-4
13. Xu DK, Lu B, Cao TT, Zhang H, Chen J, Long H, Cao J (2016) Enhancement of process capabilities in electrically-assisted double sided incremental forming. Mater Des 92:268–280. https://doi.org/10.1016/j.matdes.2015.12.009
14. Honarpisheh M, Abdolhoseini MJ, Amini S (2016) Experimental and numerical investigation of the hot incremental forming of Ti-6Al-4V sheet using electrical current. Int J Adv Manuf Technol 83(9):2027–2037. https://doi.org/10.1007/s00170-015-7717-7
15. Najafabady SA, Ghaei A (2016) An experimental study on dimensional accuracy, surface quality, and hardness of Ti-6Al-4 V titanium alloy sheet in hot incremental forming. Int J Adv Manuf Technol 87(9):3579–3588. https://doi.org/10.1007/s00170-016-8712-3
16. Liu R, Lu B, Xu D, Chen J, Chen F, Ou H, Long H (2016) Development of novel tools for electricity-assisted incremental sheet forming of titanium alloy. Int J Adv Manuf Technol 85(5):1137–1144. https://doi.org/10.1007/s00170-015-8011-4
17. Magnus CS (2017) Joule heating of the forming zone in incremental sheet metal forming: part 1. Int J Adv Manuf Technol 91(1):1309–1319. https://doi.org/10.1007/s00170-016-9786-7
18. Pacheco PAP, Silveira ME (2018) Numerical simulation of electric hot incremental sheet forming of 1050 aluminum with and without preheating. Int J Adv Manuf Technol 94(9):3097–3108. https://doi.org/10.1007/s00170-017-0879-8